

Hydrographic Survey of Columbia Bay, October 8-11 2014.

December 15, 2014

A report prepared for the Regional Citizen's Advisory Council under contract number
8551.14.01

Robert W. Campbell, Ph.D.
Prince William Sound Science Center
PO Box 705
Cordova, AK
99574
rcampbell@pwssc.org

The opinions expressed in this PWSRCAC-commissioned report are not necessarily those of
PWSRCAC

Abstract

A hydrographic survey of Columbia Bay was conducted in early October 2014, to survey the nascent fjord created by the retreat of Columbia Bay. Hydrographic sections show the characteristic pattern created by tidewater glaciers, with a surface and subsurface freshwater plume near the face of the glacier, with the coldest and freshest waters occurring in the vicinity of the relatively new western face. Very high turbidities were also observed in the vicinity of the calving faces. Reduced salinity and turbidity near-bottom in some locations suggests that there may be sub-bottom sources of fresh water as well. Examination of the water properties near the face show the importance of ice melt in creating the water masses within the fjord basin. The melting of tremendous amounts of ice in the last 40 years has led to a cooling and freshening of the waters in the basin.

Introduction

Columbia Bay is a relatively new fjord adjacent to Prince William Sound, created when the Columbia Glacier began retreating from its terminal moraine near Heather Island in the mid-1970s. A number of oceanographic surveys were done in the vicinity of the glacier face in the early 1980s (Walters et al., 1988), when the face was approximately 1.5 kilometers north of the tip of the terminal moraine. The glacier has continued to retreat rapidly in the intervening decades, with the main face now located approximately 18 km north of the terminal moraine. The former terminal moraine is now a sill that impedes deep water mixing within the basin of the fjord. The fjord has been visited sporadically by research vessels in recent years, but most of the data collected is in the hands of individual researchers and not available. In early October 2014, staff from the Prince William Sound Science Center visited Columbia Bay aboard the M/V New Wave, to conduct a hydrographic survey of the fjord, in conjunction with a glaciological survey conducted by W.T. Pfeffer Geological Consultants. This report presents the results of that cruise.

Methods

An along-thalweg transect consisting of several hydrographic stations was conducted from beyond the terminal moraine to the main face (fig. 1). The transect was conducted twice, once in a northerly direction when entering the fjord, and again four days later when exiting. A cross-face transect was also conducted, from the western face to an eastern face below the Great Nunatak (fig. 1,2). A number of additional stations near the main face were also done. Stations near the faces were done as close as could be done safely.

At each station a CTD cast was done (a SeaBird SBE25plus with WETLabs ECO fluorometer/turbidometer, and a SeaBird SBE43 oxygen sensor), the casts were done per the following standard PWSSC protocol:

1. Following deployment, the sonde was allowed to equilibrate for at least 1 minute following pump engagement (aka a “surface soak”).
2. Prior to the cast, the ship was maneuvered such that the sonde is in clean water. The PWSSC vessel, M/V New Wave has a stern mounted A-frame used for deployment, and the

intention is to avoid having the sonde in water that has been exposed to exhaust gasses (so to avoid bubbles that will interfere with any optical instruments). This is usually accomplished by briefly placing the vessel in reverse.

3. The sonde was lowered at $0.75\text{-}1\text{ m s}^{-1}$, and vessel heave reduced as much as possible (operationally this is done with a gloved hand, which is possible because the CTD is deployed with 3/16 dyneema line).
4. The vessel was maneuvered during the cast to minimize wire angle.
5. Given the soft nature of the bottom, the sonde was lowered so as to be within 1 m of bottom. Given the depth of the fjord, there were numerous bottom touches. All were recorded in the event log for the cast, and the instruments and plumbing flushed with seawater.
6. The sonde was recovered, inspected to ensure operation (visual examination of the fluorometer LEDs), shut down, and stored according to manufacturer's recommendations. Processing of the CTD data was done as per the manufacturer's recommendations, with details of the processing steps documented in the metadata headers of the file. Processing is done with the routines provided by SeaBird electronics SBE Data Processing software, and custom software written in MATLAB. Unbinned 16 Hz observations were used in the production of this report, and salinity is reported on the PSU scale. Pressure measurements from the CTD were converted to depth, and *in situ* density computed with the UNESCO algorithms (UNESCO, 1983). Density is reported in 'sigma' units, which is the density in kg m^{-3} minus 1000. Turbidity measurements are notoriously difficult, and the turbidometer used here was not designed for extremely turbid waters – turbidity is reported as voltage from the sensor (which has a linear response), and the maximum value is 5 volts. Near the glacier face, the instrument tended to peg at 5 volts in the high turbidity water.

The CTD and Oxygen sensor are calibrated annually (the last calibration was January 2014, the instruments are being recalibrated at the time this report is being written). Interannual drift of the instruments is generally low (in the third decimal place), in the event that drifts are large, the data may be post-processed to account for the drift. Winkler titrations were not done to calibrate the oxygen sensor, so oxygen values should be viewed as only semi-quantitative (but can be expected to be internally consistent).

Sections of the hydrographic quantities (temperature, salinity, turbidity, oxygen) were produced by interpolating the casts onto a regular grid (0.5 m in the vertical and 0.1 km in the horizontal) with linear interpolation. The interleaving and mixing of fresh and salt water results in rather high frequency variability in the 16 Hz CTD observations, and this tends to create artifacts in the resulting contours. Those artifacts have been left in, and the reader should make note of the positions of the stations (i.e. where there is data) when interpreting the figures.

Results/Discussion

Along thalweg transect: The results of the hydrographic survey were in line with what one might expect from a fjord with a tidewater glacier. Inside the sill, the waters of the fjord were cooler (figs 3,4,5) and fresher (figs 6,7,8) than the outside waters. A tongue of cold fresh water at the surface extended well away from the glacier face, and a cool, fresh layer extended beyond the sill. Currents were not measured during the survey, but it is likely that there was an outflow at the surface of those cool, fresher waters, and an inflow of comparatively warmer and fresher water at depth, as generally occurs at sills (Pickard, 1979; Walters et al., 1988).

The October 8 transect terminated some distance from the main face of the glacier (~500m), because the safety of working near the face had not yet been determined. A number of stations were done closer to the face on October 9, and the outgoing transect on October 11 started very close to the face (~60 m), and with several stations done near the face, which permits a close-up view of the melting dynamics near the face. Temperature (fig. 3) and salinity (fig. 8) sections both show a subsurface plume of cool, fresh water emanating from the base of the glacier face, in addition to a thin layer of cold, fresh water at the surface. The plume is caused by convective mixing of meltwater from the glacier (Motyka et al., 2013). There was also some indication of freshwater inputs at the bottom in the main basin in the October 8 transect (fig. 6), which also appeared in the turbidity section (see below).

It is not possible to extract tidal information from the two transects, each took in excess of one tidal cycle to complete. There are however some obvious differences between the two transects in terms of the depths of some of the isotherms and isohalines: The difference between the transects may be visualized by calculating the difference in temperature and salinity by subtracting one interpolated grid from the other (at those locations where both the grids line up). Sections of those differences show large departures in temperature (fig. 9) and salinity (fig. 10). Some of those differences are likely from high frequency variability (e.g. tides), but several of the excursions are quite large (2-3 °C and 1-1.5 salinity units) and span order ten meters in depth. They likely reflect variability in inputs from the glacier, and larger scale oceanographic features (e.g. internal waves and seiches within the basin).

The backscatter turbidometer showed a dense plume of very turbid water extending well away from the glacier face (figs 11, 12). Some of the casts also showed a decrease in turbidity near bottom (both the along thalweg and cross-face transects, see below), which matched up with observations of lowered salinities; this may indicate the presence of freshwater springs in the bottom of the fjord (discussed below).

Oxygen concentrations were also different within the fjord (figs 13,14), with more highly oxygenated water near the glacier face and at depth, compared to decreasing oxygen concentrations with depth outside the sill (deep waters of PWS are often ~50% of saturation).

The October 8 transect showed lower oxygen concentrations near bottom, while the October 11 transect did not, perhaps because of small variations in the positions of the stations.

Cross-face transect: The cross-face transect showed another glacier melt plume at the western face made up of cold, relatively fresh water (figs 15 and 16). Turbidity was elevated in the plume (fig 17), and lower near the surface, which was different from the situation at the main face, and may reflect differences in the size and path of the two glaciers (there is much more ice feeding the main face). There was also another location near the base of the glacier with reduced salinity and turbidity, indicating perhaps another location with sub-bottom water inputs (see below). Oxygen was also quite low in that location (fig 18), but otherwise did not vary greatly across the basin. The eastern face was much shallower than the western face and behind a small sill. That portion of the glacier is quite thin, and appears to be melting in place and not advancing; no plume was evident along that face, only weak temperature and salinity stratification. The cast closest to the western face had the coldest temperatures and salinities observed near the faces, which is likely do in part to the confined nature of that portion of the basin. It is also possible that the incoming freshwater is sets up a geostrophic circulation within the head of the bay, that would tend to transport water from the main face towards the western face (observations of ice circulation may confirm this). Prevailing winds during the survey were also from the north, which would tend to enhance westward transport (much of the surface ice was located along the western side of the inlet).

Temperature-salinity properties near the faces: Profiles of temperature and salinity from casts done near the faces, along with a cast done midway down the thalweg (but inside the sill), and the most southerly cast are shown in fig. 19, and show how temperature and salinity increase as one moves away from the glacier face. The temperature-salinity properties of the water may be used to infer the sources of water to the bay (fig. 19, right panel; adiabatic lapse has been ignored given the relatively shallow depths). When ice melts in water, the latent heat of melting results in a large change in temperature relative to salinity (Gade, 1979), resulting in a characteristic low temperature and low salinity water mass. The trajectory of melting ice in temperature-salinity space may be estimated with a simple model (Gade, 1979):

$$\frac{dT}{dS} = \left[(T_s - T_f) + \frac{c_i}{c_w} (T_f - T_i) + \frac{L}{c_w} \right] S_s^{-1}$$

Where T_s and S_s are the temperature and salinity of the source waters, T_f is the interface freezing temperature (estimated as -1.5 for seawater), T_i is the internal temperature of the ice (estimated as 0°C) c_i and c_w are the specific heat for water and ice, and L is the latent heat of fusion. Assuming source waters of $T_s=8.6^\circ\text{C}$ and $S_s=28.4$, dT/dS is 3.14, and is indicated by the “melt” line in figure 19. The “icewater” line in figure 19 corresponds to mixing of freshwater at 0°C (i.e. the line intersects the origin, and $dT/dS= T_s/S_s$).

The TS diagram (fig 19, right panel) indicates that the waters near the face are a combination of both ice melt, and meltwater that is transported through the glacier. This analysis was done by

Walters et. al (1988) with data from August 1984, when the face was much closer to the moraine, but with similar results. Their slope of dT/dS for ice was also 3.14, but the source waters were different ($T_s=11.5^\circ\text{C}$ and $S_s=29.3$). The warmer temperatures are likely due to the time of year, but it is interesting to note that the TS diagram presented by Walters et al. (1988) is shifted relative to that of fig. 19, and is about 4°C colder and 3 salinity units fresher. That shift suggests that the tremendous amount of ice mass lost as the fjord has grown, along with the restriction in mixing created by the sill, has created a water mass that is much cooler and fresher than the waters of Prince William Sound.

Sub-bottom water sources – are there freshwater springs in the bottom of the basin?

Columbia Bay is a challenging location in which to work: the bottom is extremely irregular, and it is difficult to lower the CTD to very near the bottom without touching, in attempting to sample the entire water column, a number of bottom touches occurred (the bottom is primarily fine muds, and does not endanger the instruments, though it is very important to clean the plumbing thoroughly after a bottom touch). The turbidometer used in this study is a backscatter type (Boss and Pegau, 2001), and is mounted in a downward looking configuration. The length scale of the beam (i.e. the distance the instrument “sees”) is order of 30 cm: Bottom touches in clear water thus register as an increase in turbidity caused by the sensor imaging the bottom. The CTD processing routines used here are specifically designed to permit detection of that characteristic turbidity increase and to remove it. It became apparent during the processing that at a number of stations, there were decreases in turbidity near the bottom. Upon closer inspection, it was found that those increases in turbidity usually accompanied a decrease in salinity and temperature (fig 20). Profiles of density also indicate instability (less dense water under more dense), which suggests that there are seeps of fresh, clear water entering into the bottom of the basin, that are mixing with the saltier water above. Subsurface freshwater seeps and subsurface estuaries have been observed (Li et al., 2004), but this appears to be the first documented case in the vicinity of a tidewater glacier.

Literature cited

- Boss, E. and W.S. Pegau. 2001 . “Relationship of light scattering at an angle in the backward direction to the backscattering coefficient. *Appl. Optics*. 40:5503-5507.
- Gade, H.G. 1979. Melting of ice in sea water: a primitive model with application to the Antarctic Ice Shelf and ice bergs. *J. Phys. Oceanogr.* 9:189-198.
- Li, L., Barry, D.A., Jeng, D.-S., and H. Prommer. 2004. Tidal dynamics of groundwater flow and contaminant transport in coastal aquifers. Pp. 115-141 *in*: A. H.-D. Cheng and D. Ouazar (eds). *Coastal Aquifer Management-Monitoring, Modeling, and Case Studies*. Lewis Publishers, Boca Raton, FL.
- Motyka, R.J., Dryer, W.P., Amundson, J., Truffer, M., and A. Fahnestock. 2013. Rapid submarine melting driven by subglacial discharge, LeConte Glacier, Alaska. *Geophys. Res. Lett.* 40:5153–5158, doi:10.1002/grl.51011, 2013
- Pickard, G.L. 1967. Some oceanographic characteristics of the larger inlets of Southeast Alaska. *J. Fish. Res. Bd. Can.* 24:1475-1505.
- Unesco 1983. Algorithms for computation of fundamental properties of seawater. Unesco Tech. Pap. Mar. Sci. No. 44, 53 pp.
- Walters, R. A., Josberger, E.G, and C. L. Driedger. 1988. Columbia Bay, Alaska: An “upside down” estuary, *Estuarine Coastal Shelf Sci.* 26:607–617.

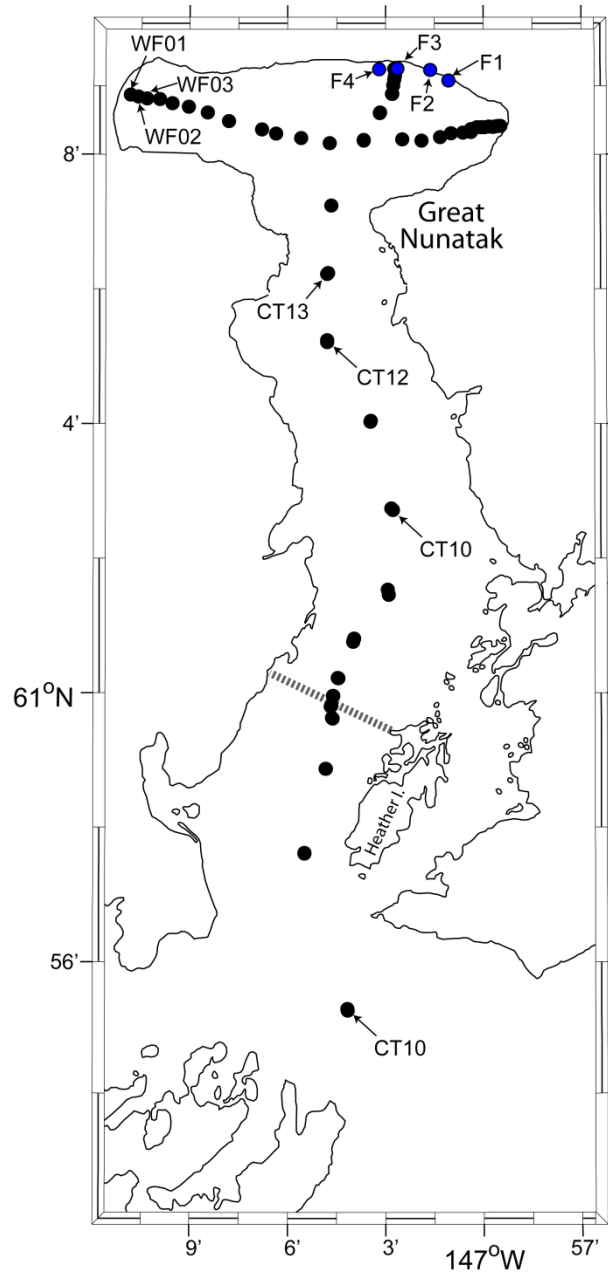


Figure 1: Map of the survey location and hydrographic stations. Geographic features and stations specifically referenced are identified. The dashed grey line indicates the approximate position of the sill.

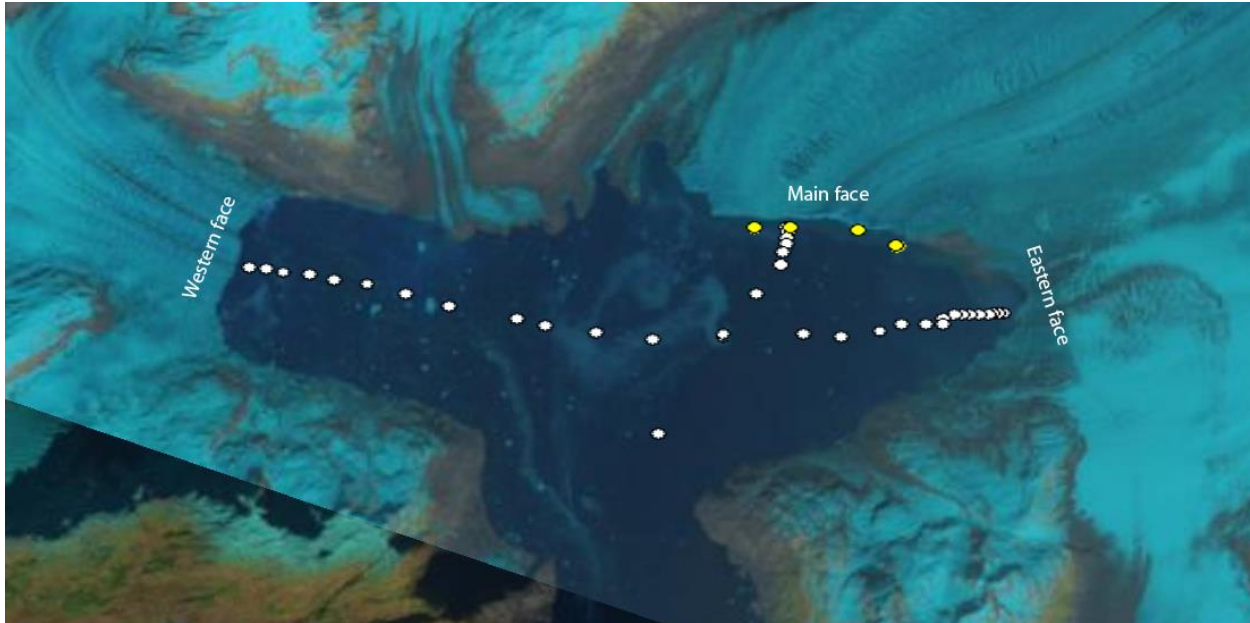


Figure 2: Approximate position of stations occupied at the head of the bay, overlaid on a Landsat-8 image taken October 13, 2014. The faces referred to in the text are indicated. White symbols denote stations occupied during the transects, and yellow stations are stations done along the face.

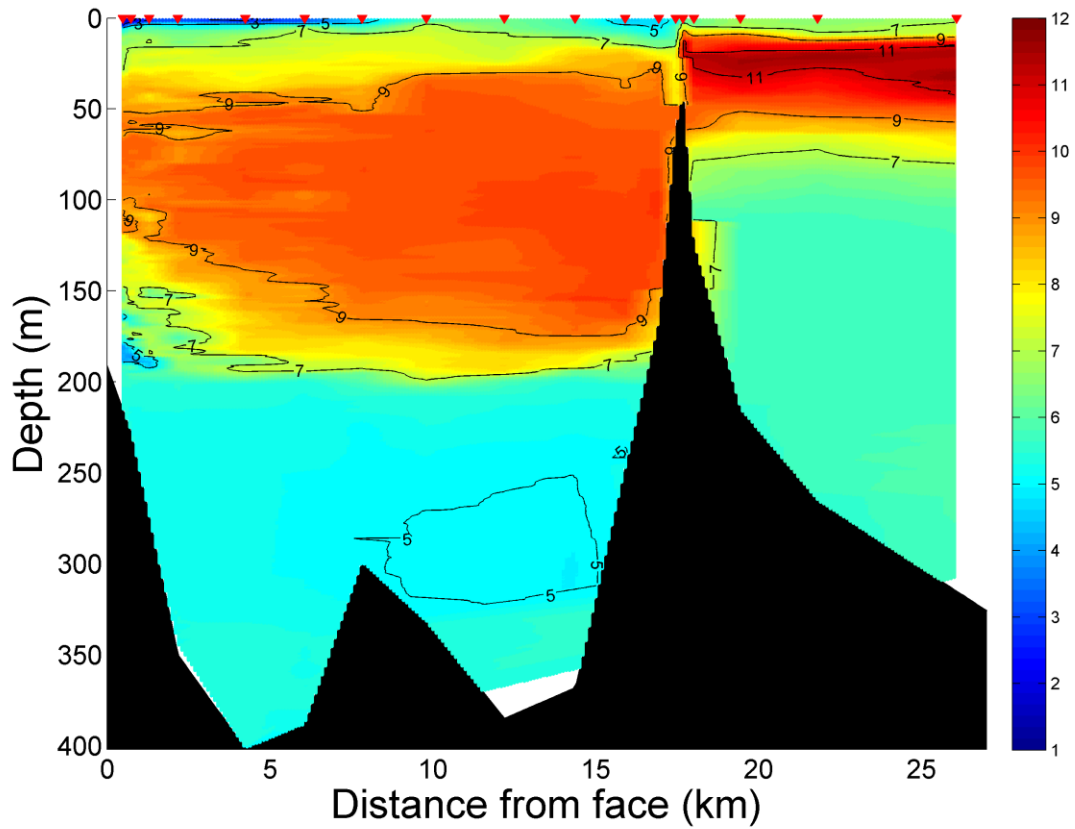


Figure 3: Temperature ($^{\circ}\text{C}$) section of the along-thalweg transect done October 8 2014. Red triangles denote station locations, and the bottom is indicated in black. Cast data were linearly interpolated on to a $0.5\text{ m} \times 0.1\text{ km}$ grid to produce the contours and heat map. The zero point is the approximate position of the main face of the glacier.

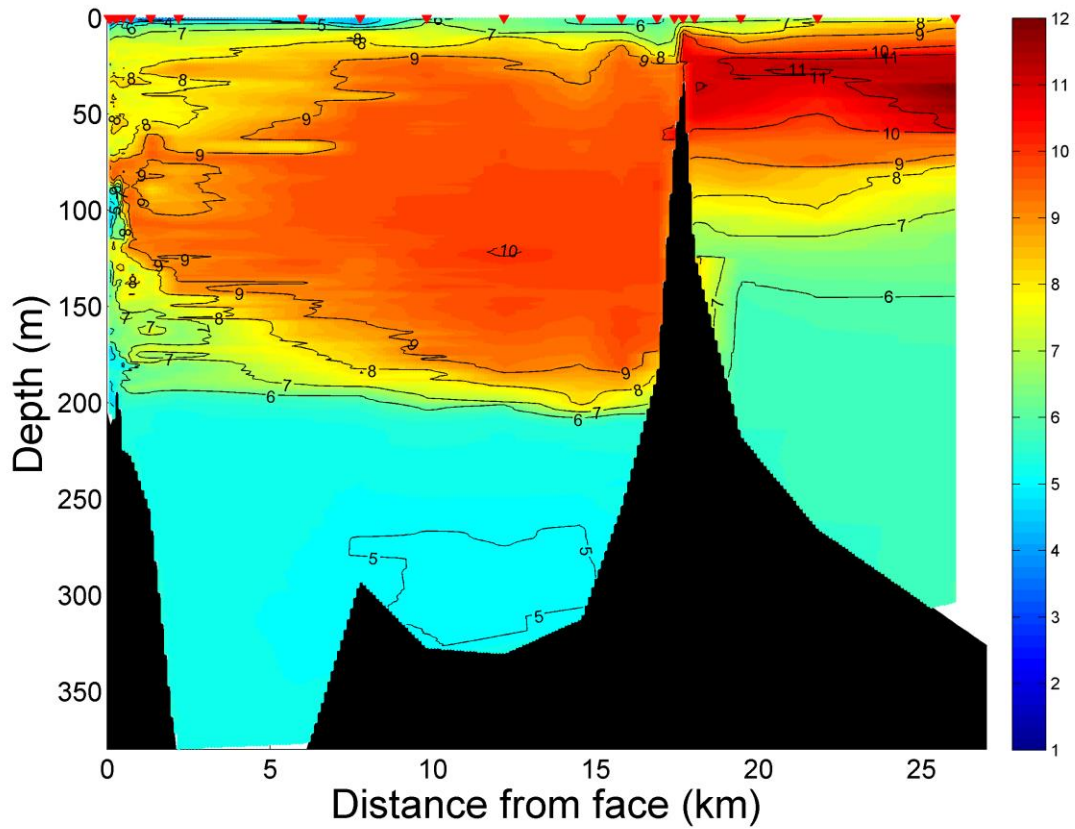


Figure 4: Temperature ($^{\circ}\text{C}$) section of the along-thalweg transect done October 11 2014. Red triangles denote station locations, and the bottom is indicated in black. Cast data were linearly interpolated on to a $0.5\text{ m} \times 0.1\text{ km}$ grid to produce the contours and heat map. The zero point is the approximate position of the main face of the glacier.

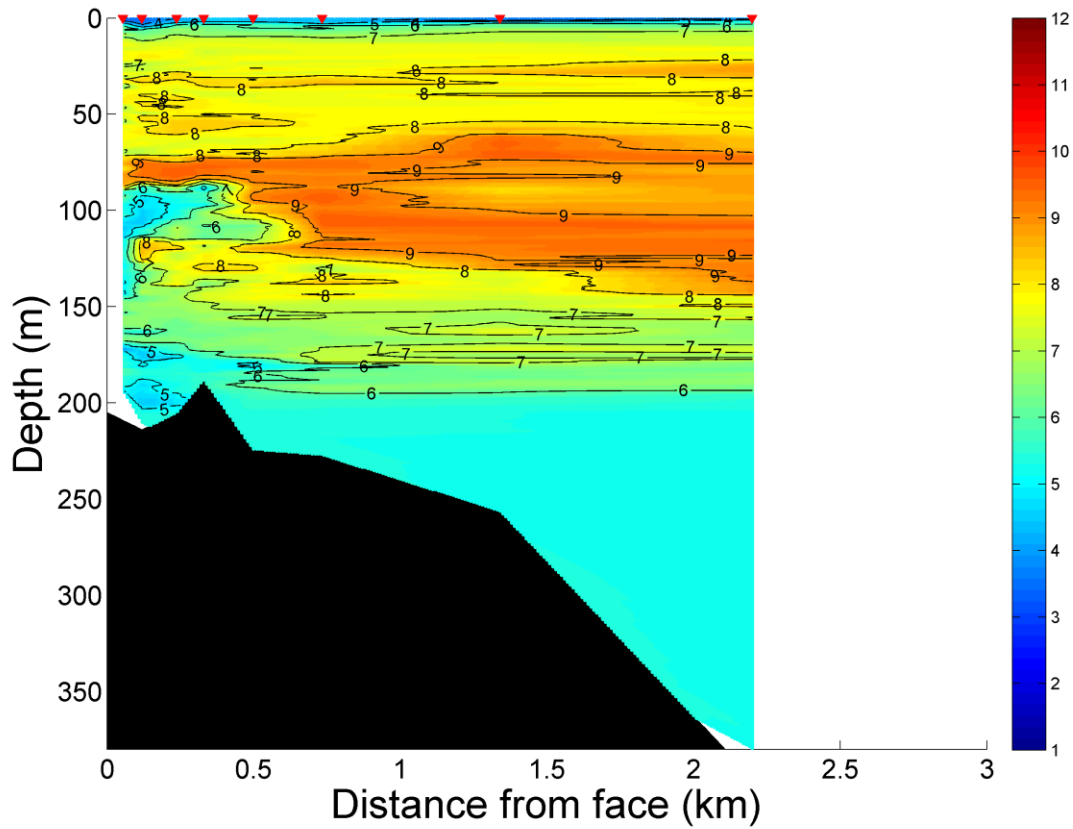


Figure 5: Close-up of the temperature ($^{\circ}\text{C}$) section of the along-thalweg transect done October 11 2014 in the vicinity of the main face (i.e. same data as fig. 4, but zoomed in to the area of the main face). Red triangles denote station locations, and the bottom is indicated in black. Cast data were linearly interpolated on to a $0.5\text{ m} \times 0.1\text{ km}$ grid to produce the contours and heat map. The zero point is the approximate position of the main face of the glacier.

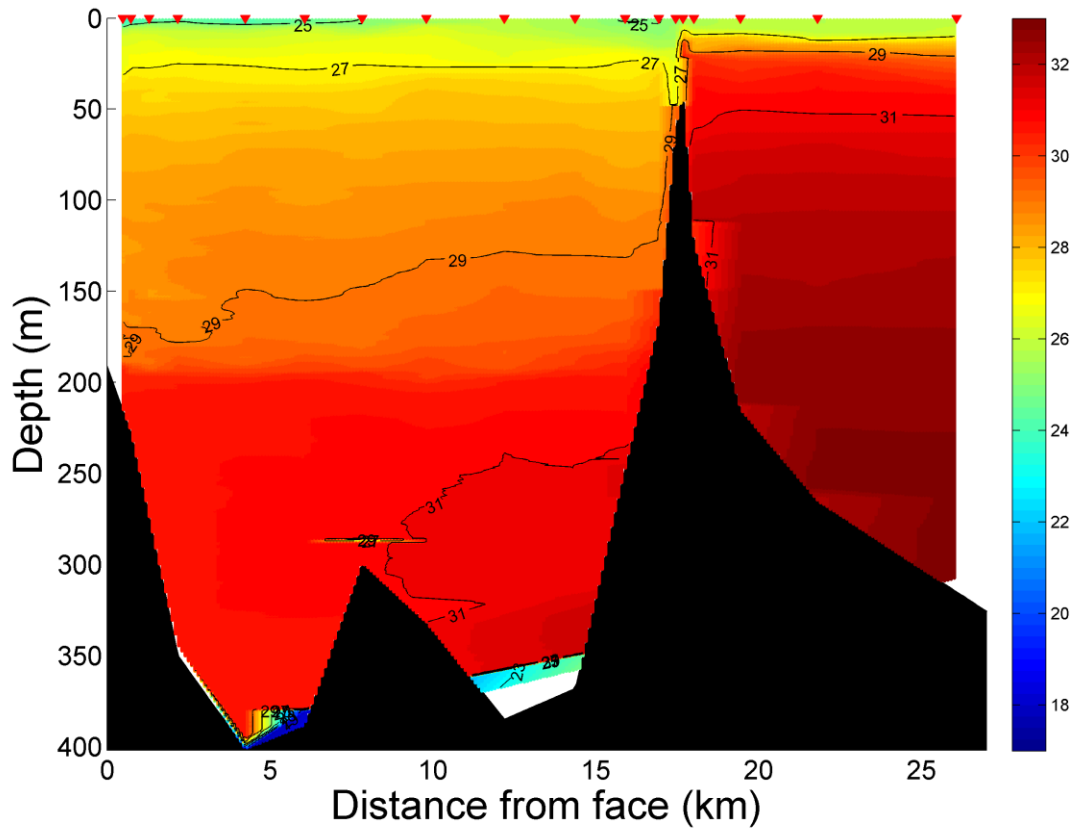


Figure 6: Salinity section of the along-thalweg transect done October 8 2014. Red triangles denote station locations, and the bottom is indicated in black. Cast data were linearly interpolated on to a 0.5 m x 0.1 km grid to produce the contours and heat map. The zero point is the approximate position of the main face of the glacier.

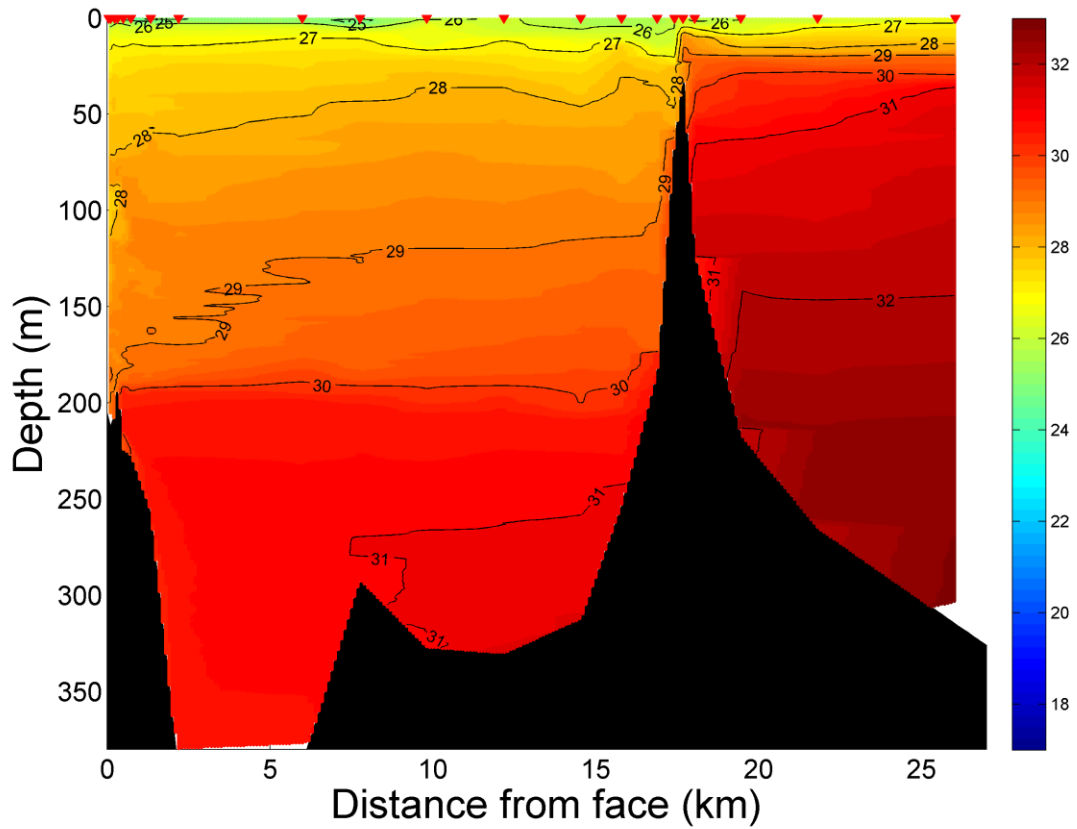


Figure 7: Salinity section of the along-thalweg transect done October 11 2014. Red triangles denote station locations, and the bottom is indicated in black. Cast data were linearly interpolated on to a 0.5 m x 0.1 km grid to produce the contours and heat map. The zero point is the approximate position of the main face of the glacier.

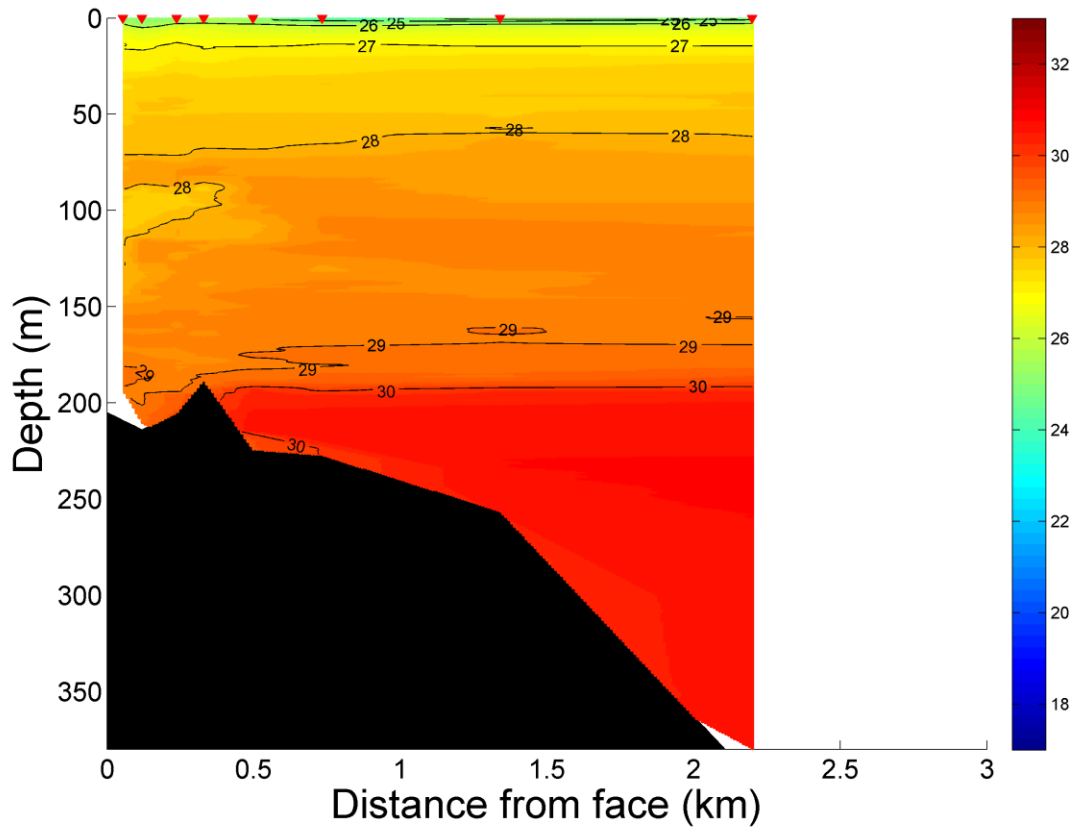


Figure 8: Close-up of the salinity section of the along-thalweg transect done October 11 2014 in the vicinity of the main face (i.e. same data as fig. 7, but zoomed in to the area of the main face). Red triangles denote station locations, and the bottom is indicated in black. Cast data were linearly interpolated on to a 0.5 m x 0.1 km grid to produce the contours and heat map. The zero point is the approximate position of the main face of the glacier.

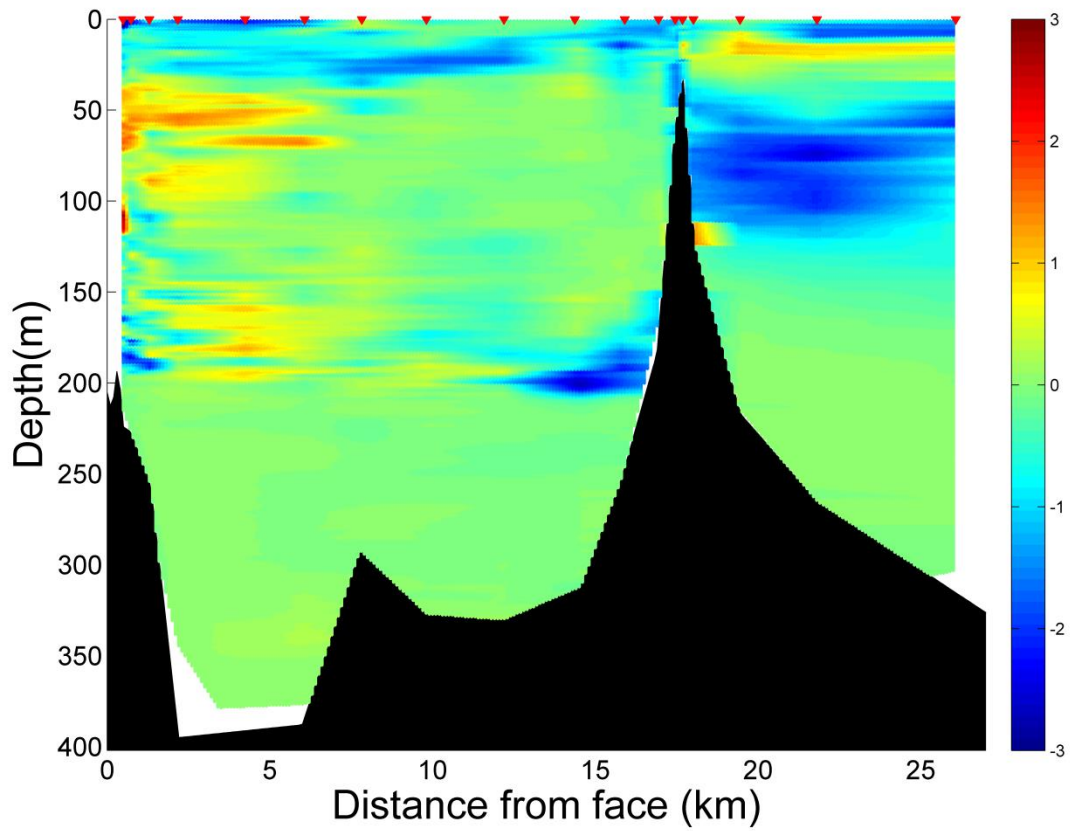


Figure 9: Heat map of differences in temperature ($^{\circ}\text{C}$) between the October 8 and October 11 transects. The heat map was produced by subtracting the October 11 grid (fig. 4) from the October 8 grid (fig. 3).

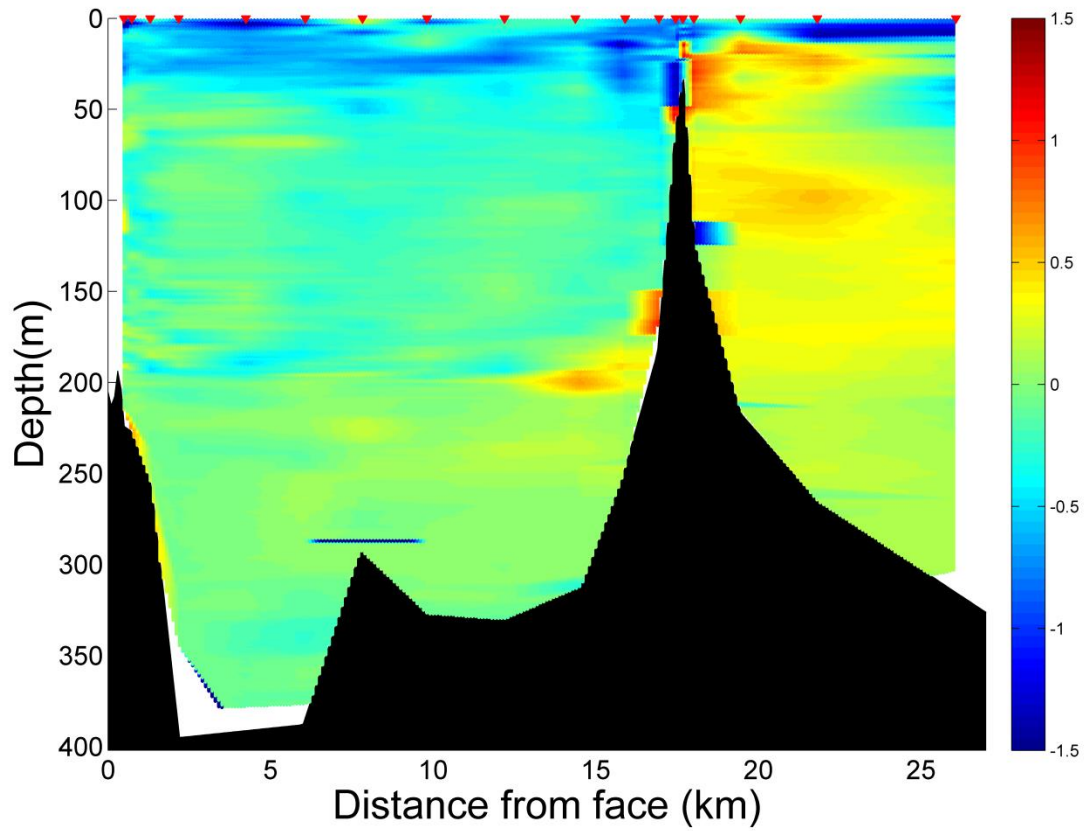


Figure 10: Heat map of differences in salinity between the October 8 and October 11 transects. The heat map was produced by subtracting the October 11 grid (fig. 7) from the October 8 grid (fig. 6).

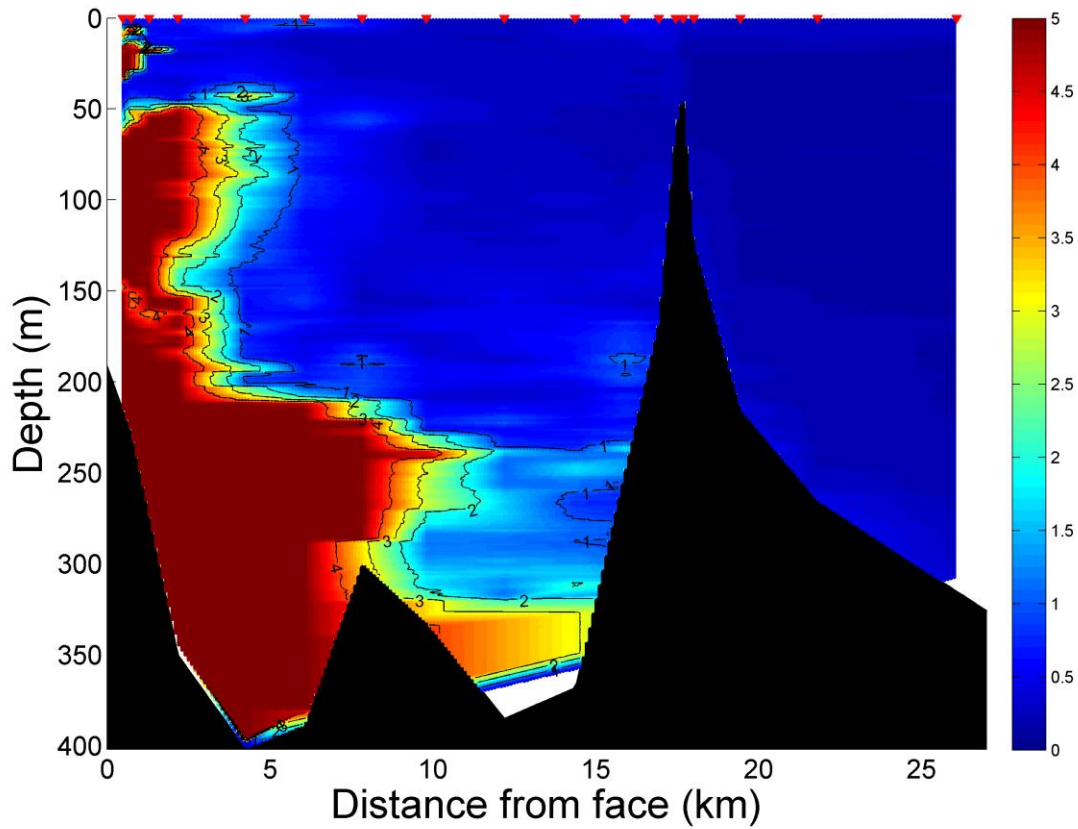


Figure 11: Turbidity (volts) section of the along-thalweg transect done October 8 2014. Red triangles denote station locations, and the bottom is indicated in black. Cast data were linearly interpolated on to a 0.5 m x 0.1 km grid to produce the contours and heat map. The zero point is the approximate position of the main face of the glacier.

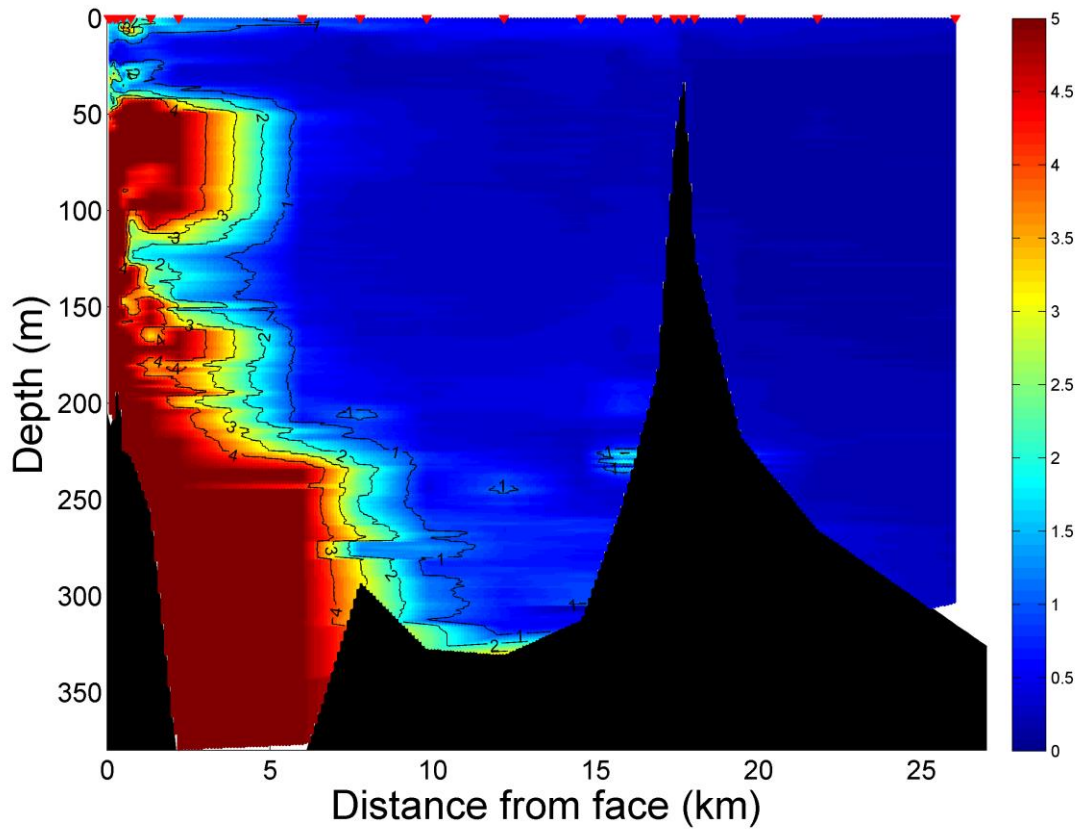


Figure 12: Turbidity (volts) section of the along-thalweg transect done October 11 2014. Red triangles denote station locations, and the bottom is indicated in black. Cast data were linearly interpolated on to a 0.5 m x 0.1 km grid to produce the contours and heat map. The zero point is the approximate position of the main face of the glacier.

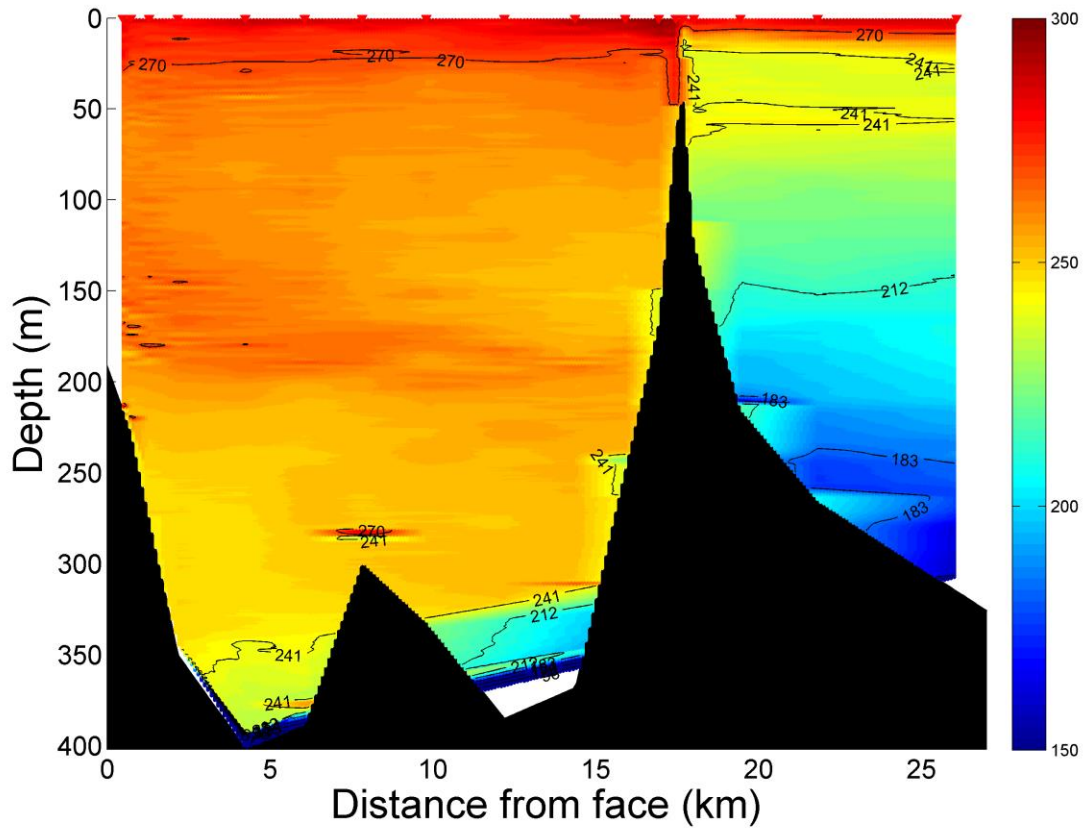


Figure 13: Oxygen ($\mu\text{mol kg}^{-1}$) section of the along-thalweg transect done October 8 2014. Red triangles denote station locations, and the bottom is indicated in black. Cast data were linearly interpolated on to a $0.5 \text{ m} \times 0.1 \text{ km}$ grid to produce the contours and heat map. The zero point is the approximate position of the main face of the glacier.

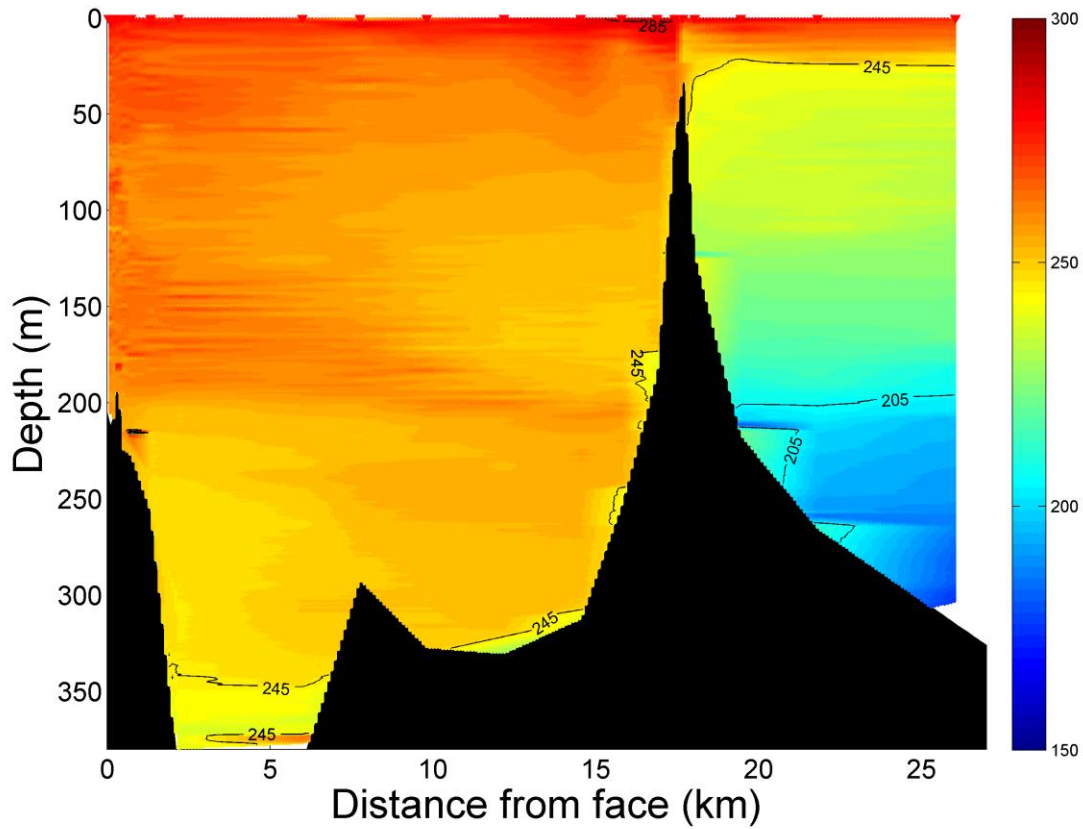


Figure 14: Oxygen ($\mu\text{mol kg}^{-1}$) section of the along-thalweg transect done October 11 2014. Red triangles denote station locations, and the bottom is indicated in black. Cast data were linearly interpolated on to a $0.5 \text{ m} \times 0.1 \text{ km}$ grid to produce the contours and heat map. The zero point is the approximate position of the main face of the glacier.

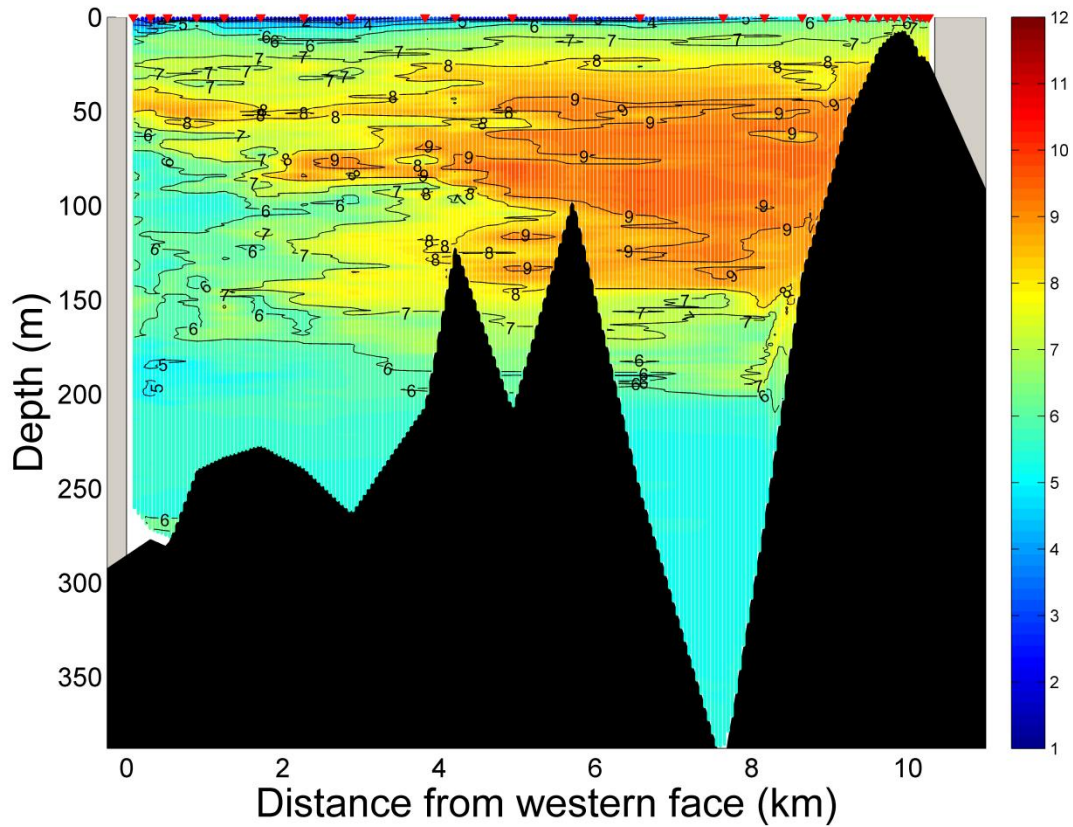


Figure 15: Temperature ($^{\circ}\text{C}$) section of the cross-face transect. Red triangles denote station locations, and the bottom is indicated in black. Cast data were linearly interpolated on to a $0.5\text{ m} \times 0.1\text{ km}$ grid to produce the contours and heat map. The zero point is the approximate position of the western face of the glacier, and the grey boxes indicate the approximate positions of the glaciers.

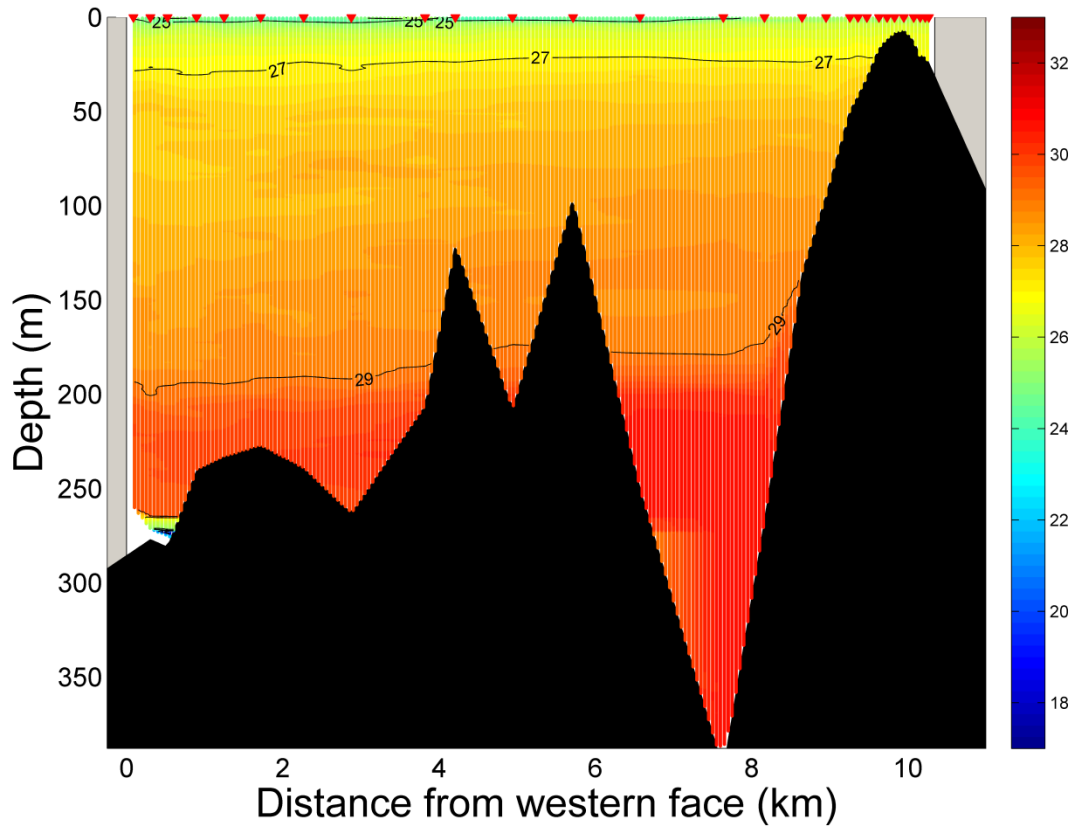


Figure 16: Salinity section of the cross-face transect. Red triangles denote station locations, and the bottom is indicated in black. Cast data were linearly interpolated on to a 0.5 m x 0.1 km grid to produce the contours and heat map. The zero point is the approximate position of the western face of the glacier, and the grey boxes indicate the approximate positions of the glaciers.

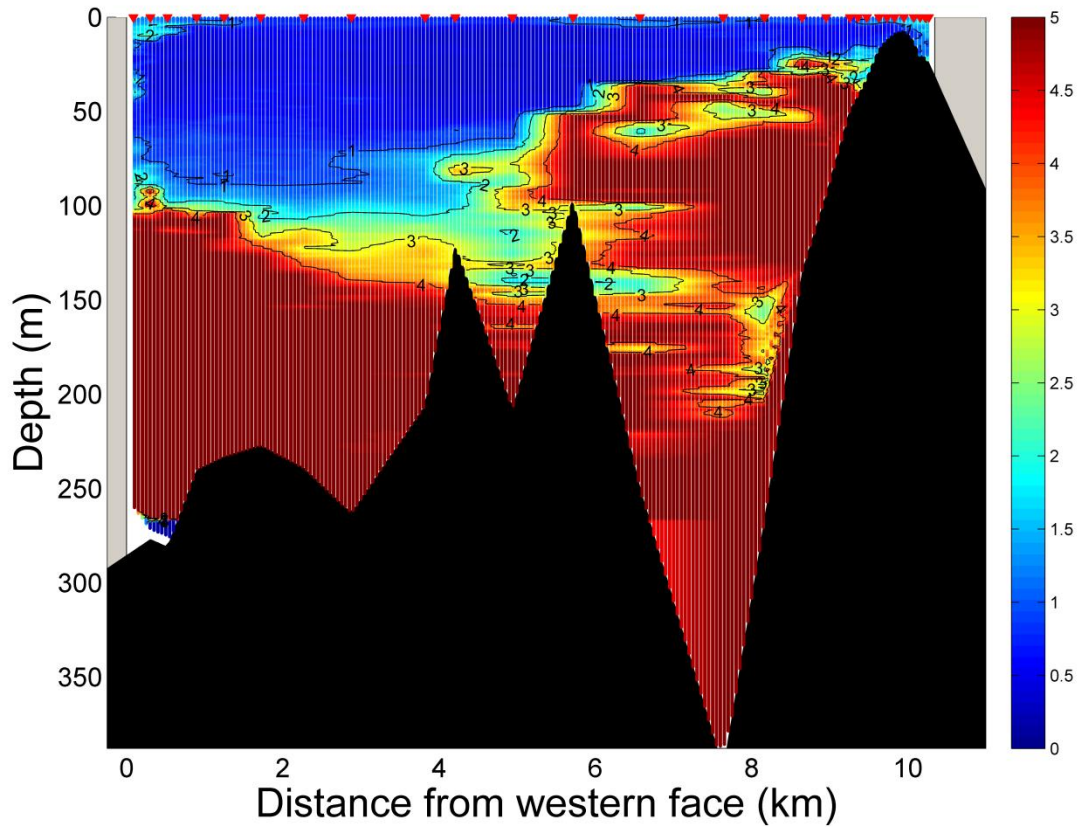


Figure 17: Turbidity (volts) section of the cross-face transect. Red triangles denote station locations, and the bottom is indicated in black. Cast data were linearly interpolated on to a 0.5 m x 0.1 km grid to produce the contours and heat map. The zero point is the approximate position of the western face of the glacier, and the grey boxes indicate the approximate positions of the glaciers.

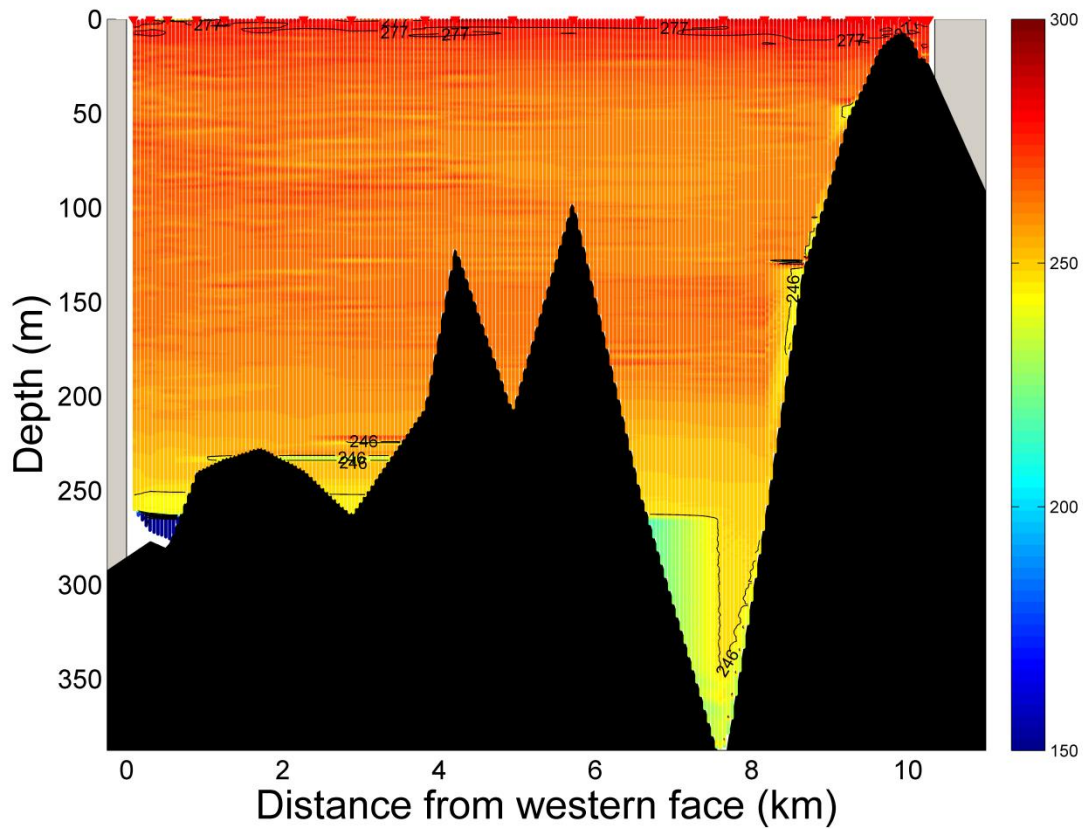


Figure 18: Oxygen ($\mu\text{mol kg}^{-1}$) section of the cross-face transect. Red triangles denote station locations, and the bottom is indicated in black. Cast data were linearly interpolated on to a 0.5 m x 0.1 km grid to produce the contours and heat map. The zero point is the approximate position of the western face of the glacier, and the grey boxes indicate the approximate positions of the glaciers.

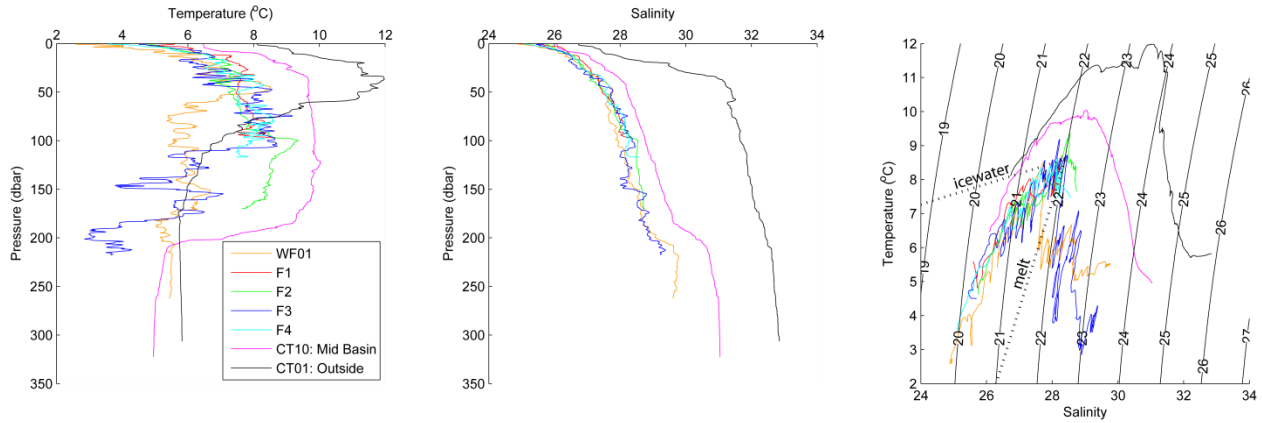


Figure 19: Left panel: Temperature profiles from a number of the near-face casts, along with a station midway down the basin but inside the sill (CT10: see fig. 1), and the outermost station outside of the sill (CT01). Middle panel: Salinity profiles from the same stations as the left panel. Right panel: T-S diagram from the same stations as the other panels. The contours are lines of constant density (in sigma units). The ‘icewater’ line is the mixing line for mixing salt water with fresh water at 0°C, and the ‘melt’ line is for ice melting in seawater.

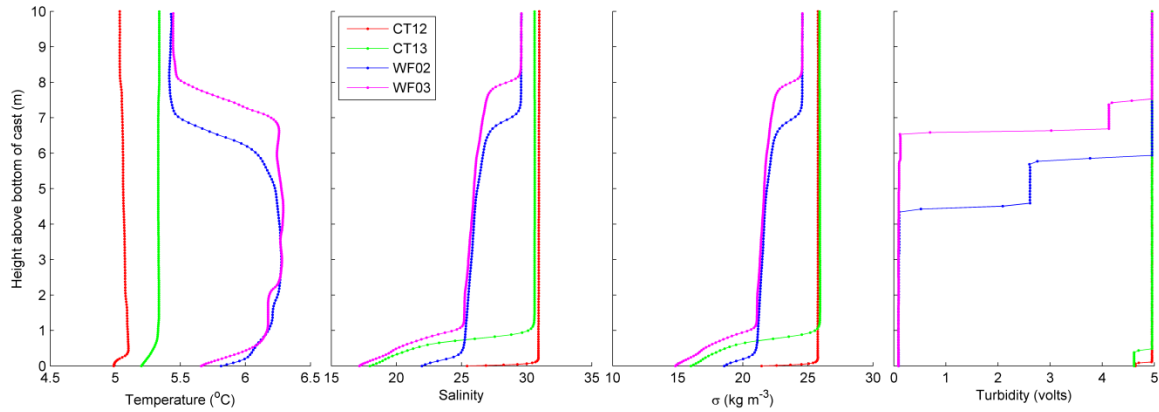


Figure 20: Near-bottom profiles of temperature (1st panel), salinity (2nd panel), density (3rd panel) and turbidity (4th panel), at stations suggestive of freshwater inputs from the bottom. Each cast had a different cast depth, so each cast was scaled to show distance above the bottom of the cast so that all could be plotted together. Density is shown in sigma units (density – 1000).